

Clustering, Order, and Collapse in a Driven Granular Monolayer

J. S. Olafsen* and J. S. Urbach

Department of Physics, Georgetown University, Washington, D.C. 20057

(Received 3 June 1998)

Steady state dynamics of clustering, long-range order, and inelastic collapse are experimentally observed in vertically shaken granular monolayers. At large vibration amplitudes, particle correlations show only short-range order like equilibrium 2D hard sphere gases. Lowering the amplitude “cools” the system, resulting in a dramatic increase in correlations leading to either clustering or an ordered state. Further cooling forms a collapse: a condensate of motionless balls coexisting with a less dense gas. Measured velocity distributions are non-Gaussian, showing nearly exponential tails. [S0031-9007(98)07625-X]

PACS numbers: 46.10.+z, 05.70.Ln, 64.60.Qb, 83.10.Pp

Granular systems exhibit static and dynamic disorder [1], inviting a statistical description. Results of equilibrium statistical mechanics are not directly applicable to excited granular systems, however, due to the large dissipation during collisions. In particular, the phenomena of clustering and collapse in a freely cooling, initially homogeneous granular medium are examples of nonuniform energy distributions arising from instabilities in the collective motion as energy is lost through interparticle collisions [2–5]. The instabilities lead to clusters, regions of high particle density and increased dissipation rate. The continued dissipation of energy in the freely cooling case eventually leads to inelastic collapse, where two or more particles lose all relative motion [3]. By contrast, in an isochoric equilibrium elastic hard disk system particle correlations do not increase as the temperature is decreased [6].

Recent work has extended the theoretical analysis to driven systems [7–12]. The driven granular medium reaches a steady state, where the energy lost through collisions is equal to the amount added externally. By decreasing the rate of energy input, the system may be slowly cooled, maintaining the dynamics near the steady state. In this letter, we describe measurements of a large number (8000–14 500) of spherical particles on a vertically shaken, smooth horizontal plate. Unlike recent investigations of thin vertical granular layers [13,14] and a thin horizontal layer driven from one side [15], there are no large scale density gradients in this system, allowing for precise measurements of the steady state statistical properties.

The particles used in this experiment are uniform 1 mm diameter stainless steel balls [16] which constitute less than one layer coverage on a 20 cm diameter aluminum plate. As long as the shaking amplitude is not too large, the particles cannot hop over one another and the motion is effectively two dimensional (2D); the energy imparted to the vertical component of the velocity by the plate is converted into horizontal motion through the particle-particle collisions. The coefficients of restitution in this investigation are about 0.9 [17].

In these experiments, the particle-particle collision rate is on the order of the shaking frequency ω . The inter-

particle collisions destroy the delicate coherence necessary for the intermittency observed in the single sphere problem [18]. Unlike thick granular layers, where the collision rate is much higher than the shaking frequency [19], particle-plate collisions are observed throughout the plate oscillation cycle. For a vertical displacement in the shaking plate, $z(t) = A \sin(\omega t)$, the dimensionless acceleration may be defined as $\Gamma \equiv A\omega^2/g$, where g is the acceleration due to gravity. The acceleration is uniform across the plate to within 0.2%. As the system is nearly 2D, cameras placed above the plate can capture the horizontal dynamics of any particle in the system. A high resolution camera is used to measure spatial correlations in the monolayer [20] and a high speed camera to obtain particle velocities between collisions [21].

The motion is begun by shaking the plate at an acceleration where all of the particles are in motion in the gaslike phase, typically $\Gamma = 1.25$. The gas is characterized by an apparently random distribution of particle positions and velocities. Figure 1(a) is an instantaneous image of the gas for a population of 8000 particles (filling fraction $\rho = 0.463$ [16]) at $\Gamma = 1.01$ at a frequency of $\nu = \omega/(2\pi) = 70$ Hz. The bright spots are reflections on top of the particles; the particle diameter is a little more than twice the diameter of a bright spot in the instantaneous images. Figure 1(b) is a time-averaged picture of 15 frames taken over a period of 1 s, and shows the lack of any stable structure [22].

As the acceleration amplitude is slowly decreased (at constant frequency), the average kinetic energy of the particles decreases, and localized transient clusters of low-velocity particles appear. The clusters break up over a time scale of 1–20 s through interactions with higher velocity particles. Figure 1(c) is an instantaneous image when the acceleration is decreased to $\Gamma = 0.80$. To the eye, there is no significant difference from Fig. 1(a), however in the time-averaged image [Fig. 1(d)], bright peaks are clearly evident, corresponding to low-velocity particles that have remained relatively close to each other over the 1 s interval. These clusters typically extend two to three ball diameters.

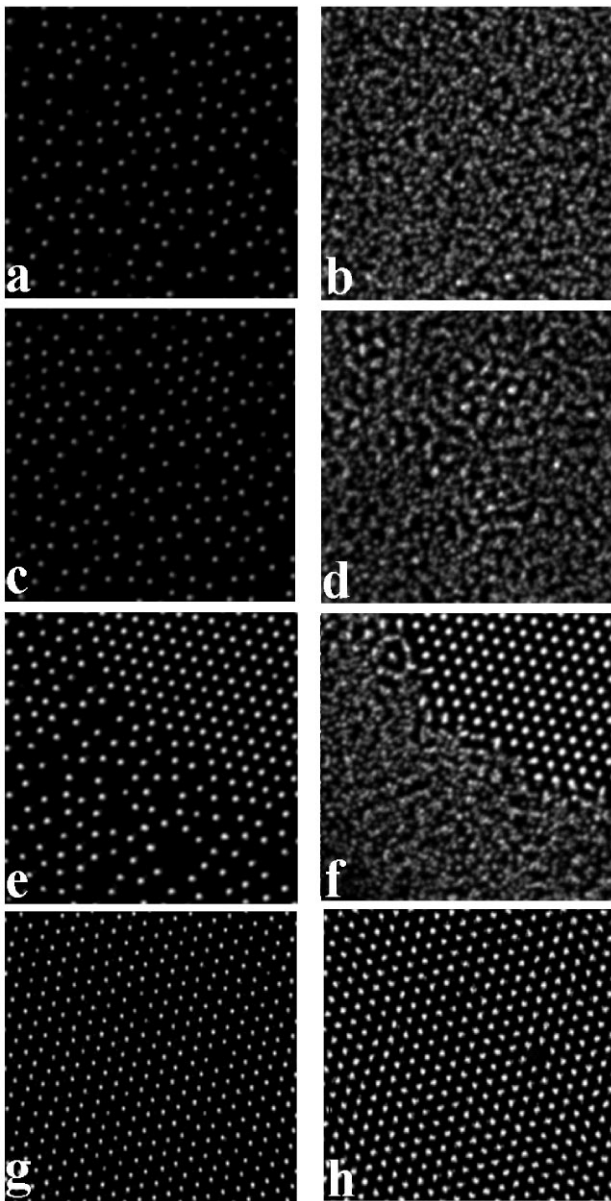


FIG. 1. Instantaneous (left column) and time-averaged (right column) photographs detailing the different phases of the granular monolayer. (a),(b) Uniform particle distributions typical of the gas phase ($\Gamma = 1.01$). (c) ($\Gamma = 0.8$) Clusters are visible as higher intensity points in a time-averaged image (d) denoting slower, densely packed particles. (e) A portion of a collapse ($\Gamma = 0.76$). (f) The time-averaged image shows that the particles in the collapse are stationary while the surrounding gas particles continue to move. (g),(h) In a more dense system, there is an ordered phase where all of the particles remain in motion.

As the acceleration amplitude is further decreased to $\Gamma = 0.76$, the typical cluster size increases to 12–15 particles. Within a few minutes at this acceleration, one of these large clusters will become a nucleation point for a collapse [23]: a condensate of particles that comes to rest on the plate while in contact with each other. The collapse reaches a steady state after several minutes,

typically forming an “island” completely surrounded by a coexisting gas. Figure 1(e) is an instantaneous image of part of a typical collapse. The particles in the close packed lattice remain in *constant* contact with each other and the plate. A similar crystalline structure has been observed in a multilayered system under horizontal shaking [24]; similar phase separation has been seen in numerical simulations [7,8]. The time-averaged image in Fig. 1(f) demonstrates that the particles in the collapse are stationary, while the particles in the coexisting gas phase are in constant motion. The two-phase coexistence persists essentially unchanged for as long as the driving is maintained.

At higher densities (increased filling fractions), instead of a transition directly from clustering behavior to collapse, there is an intermediate phase with apparent long-range order. Unlike the collapse, the particles *do not* come to rest, but fluctuate about sites arranged on a hexagonal lattice. In addition, there is no phase boundary; the ordered phase extends across the entire cell. Figures 1(g) and 1(h) show the behavior for $N = 14\,500$ ($\rho = 0.839$) and a drive frequency of 90 Hz. The hexagonal lattice is apparent in Fig. 1(g), although there is considerable positional disorder and one vacancy. That disorder is almost completely absent in the time-averaged image [Fig. 1(h)], demonstrating that the particles fluctuate about the sites on a regular lattice. The motion is visually similar to that seen in colloids [25].

Figure 2 is a “phase” diagram for two different densities. The filled circles show the acceleration Γ for which collapse forms as the gas is cooled as a function of frequency. The system is hysteretic: Once the collapse nucleates, the driving amplitude must be increased a small amount, indicated by open circles in part (a) for $N = 8000$, in order to return all of the particles to the gas phase. In part (b), results for $N = 14\,500$ are shown (for

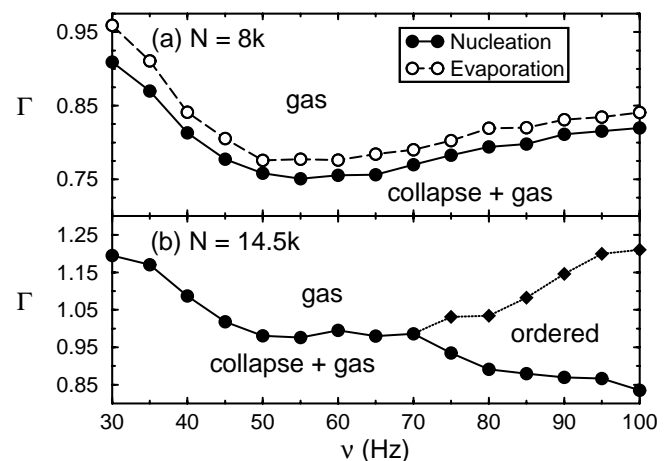


FIG. 2. The phase diagrams for (a) $N = 8000$ particles and (b) $N = 14\,500$ particles. The filled circles denote the acceleration where the collapse nucleates. The open circles in (a) indicate the point where the collapse disappears upon increasing the acceleration. The diamonds in (b) show the transition to the ordered state as the acceleration is reduced.

clarity, the evaporation line is not shown). For frequencies below 70 Hz, the cooling gas undergoes a transition to a collapse directly from a disordered phase. At frequencies above 70 Hz, the medium first undergoes a transition to an ordered state [Figs. 1(g) and 1(h)], indicated by the diamonds, and upon further cooling undergoes another transition to a collapse and coexisting gaslike phase. Both the ordered and the collapsed phases can be identified by eye.

The nature of the correlations in the gas phase is more subtle than in the collapsed or ordered phases but can be quantified. Particle positions, determined from high-resolution pictures [20], are used to calculate the particle-particle correlation function, $G(r) = \langle \rho(0)\rho(r) \rangle / \langle \rho \rangle^2$, where ρ is the particle density. In a hard sphere equilibrium gas, $G(r)$ shows no significant correlations beyond one particle diameter. The correlations are due only to geometric factors of excluded volume and are independent of temperature [6].

The solid line in Fig. 3 shows $G(r)$ from a Monte Carlo calculation of a 2D gas of elastic hard disks in equilibrium for a density of 0.463 [26]. The experimentally measured correlation function in the gaslike phase ($\Gamma = 0.892$, $\nu = 70$ Hz), shown by the open circles, is almost identical to the equilibrium result. There are no free parameters in Fig. 3. The remarkable agreement clearly demonstrates that the structure in the correlation function of the gaslike phase is dominated by excluded volume effects. As the granular medium is cooled, the correlations grow significantly. This is evident from the data for an acceleration of $\Gamma = 0.774$ (0.5% above the acceleration where collapse forms), shown as filled diamonds in Fig. 3. The increased correlations indicate that there are nonuniform density distributions in the medium: regions of high density that, due to the closed nature of the system, imply regions of low density.

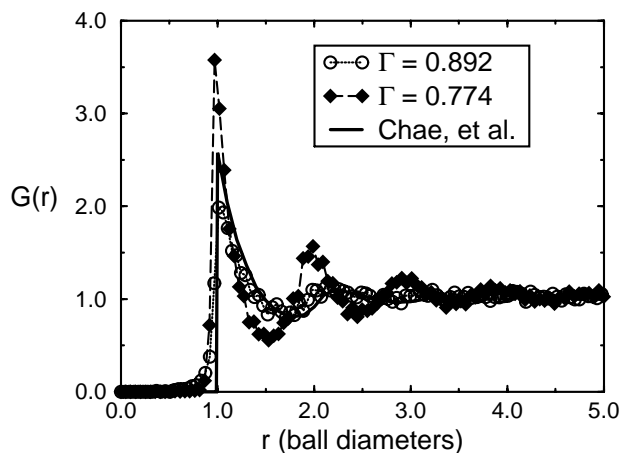


FIG. 3. Density-density correlation measurements of the granular medium. The measured correlations are compared to the result from an equilibrium hard sphere Monte Carlo calculation [26].

A crucial ingredient of a statistical approach needed to describe the dynamics in a granular system is the velocity distribution, which may show nonequilibrium effects as does the correlation function. Velocity distributions that obey Maxwell statistics have been used in the formulation of many kinetic theories of granular systems and the deviations due to inelasticity have been assumed small [2,4,5,9,12,27,28]. Recent results from simulations [7,10] and experiments [13,14] demonstrate deviations from Gaussian velocity distributions, but the experiments were not able to resolve the functional form. With the use of a high speed camera [21], the particle velocities can be determined between collisions. Extensive measurement of the velocity distributions in the plane of the granular gas in our system demonstrates non-Gaussian behavior.

Figure 4 shows that experimentally measured velocity probability distributions in the gas (circles), clustering

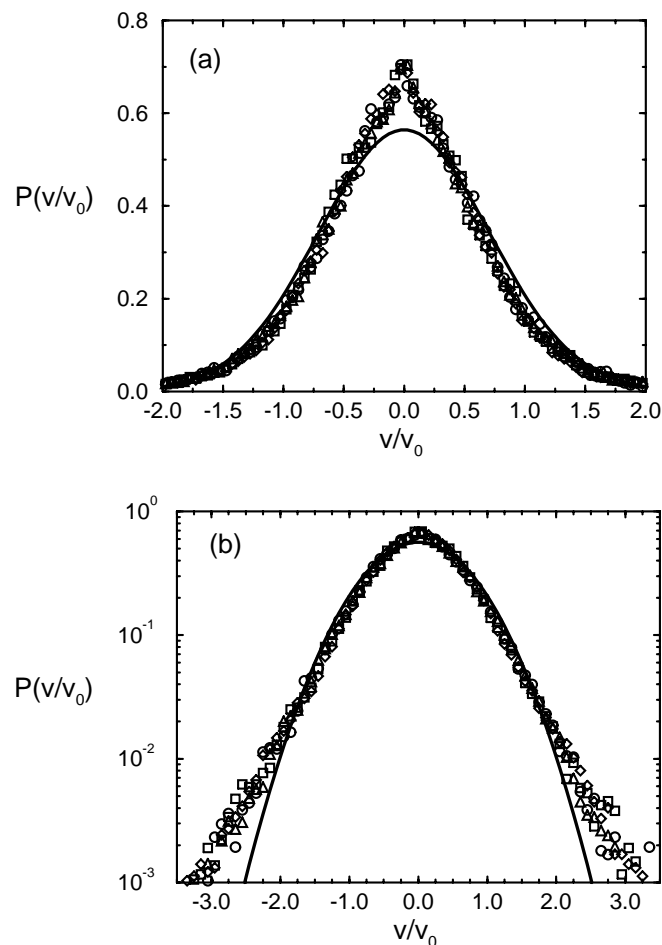


FIG. 4. Probability distribution function for a single component of the horizontal velocity on (a) linear and (b) log scales. The solid line is a Gaussian distribution. The data is (\circ) $\Gamma = 1.01$, (\square) $\Gamma = 0.80$, (\diamond) $\Gamma = 0.76$ for $N = 8000$ and $\nu = 75$ Hz; (\triangle) $\Gamma = 1.00$ for $N = 14500$ and $\nu = 90$ Hz. The large population of low-speed particles is evident in (a), while (b) shows that the tails are approximately exponential. The data is scaled by $v_0 = (2v_{2m}^2)^{1/2}$.

(squares), ordered (diamonds) phases, and the gas phase coexisting with a collapse (triangles) all deviate significantly from a Maxwellian distribution (solid line). The distributions are scaled only by a characteristic velocity $v_0 = (2v_{2m}^2)^{1/2}$ proportional to the second moment of the distribution v_{2m} and approximately follow a universal curve. As no asymmetry is observed, the distributions contain both v_x and v_y data. The second moment of the distribution varied from 3.8 cm/s in the gas phase ($\rho = 0.463$, $\Gamma = 1.01$, $\nu = 75$ Hz) to 1.5 cm/s in the ordered phase at high density ($\rho = 0.839$, $\Gamma = 1.0$, $\nu = 90$ Hz). The straight tails in Fig. 4(b) suggest an exponential velocity distribution. This result is robust: data acquired for sine, sawtooth, and square acceleration waveforms all demonstrate velocity distributions which scale onto one curve, indicating that the horizontal dynamics are dominated by particle-particle rather than particle-plate interactions.

The deviations from the Maxwell velocity distribution may result from clustering in momentum space: When the clusters form in real space they generate a local population of high-density, low-velocity particles [7]. The corresponding low-density populations are regions of decreased dissipation that allow for high-velocity particles. Thus, as seen in Fig. 4, the populations of low- and high-speed particles are higher than that expected from a Maxwell distribution, and the intermediate velocity population is less. It is interesting to note that at the acceleration where the correlation function looks like that of the equilibrium gas (Fig. 3, open circles), the velocity distribution is strongly non-Gaussian. Future work will investigate the behavior of the velocity distribution at higher accelerations and the cross correlation between the position and velocity distributions. A systematic picture of the microscopic statistics and the macroscopic phases of this simple but rich system should provide a useful test bed for theories of excited granular media.

The authors wish to acknowledge helpful conversations with Arshad Kudrolli and Jerry Gollub, and thank Harvey Gould for directing us to Ref. [26]. This work was supported by grants from the Petroleum Research Foundation and the Sloan Foundation.

*Email address: olafsen@physics.georgetown.edu

- [1] H. M. Jaeger, S. R. Nagel, and R. P. Behringer, *Rev. Mod. Phys.* **68**, 1259 (1996).
- [2] I. Goldhirsch and G. Zanetti, *Phys. Rev. Lett.* **70**, 1619 (1993).
- [3] S. McNamara and W. R. Young, *Phys. Rev. E* **53**, 5089 (1996).
- [4] T. P. C. van Noije, M. H. Ernst, R. Brito, and J. A. G. Orza, *Phys. Rev. Lett.* **79**, 411 (1997); T. P. C. van Noije, M. H. Ernst, and R. Brito, *Phys. Rev. E* **57**, R4891 (1998).
- [5] S. E. Esipov and Th. Pöschel, *J. Stat. Phys.* **86**, 1385 (1997).
- [6] L. D. Landau and E. M. Lifshitz, *Statistical Physics* (Pergamon Press, Oxford, 1980).
- [7] Y.-H. Taguchi and H. Takayasu, *Europhys. Lett.* **30**, 499 (1995).
- [8] D. R. M. Williams, *Physica (Amsterdam)* **233A**, 718 (1996).
- [9] B. C. Eu and H. Farhat, *Phys. Rev. E* **55**, 4187 (1997).
- [10] E. L. Grossman, T. Zhou, and E. Ben-Naim, *Phys. Rev. E* **55**, 4200 (1997).
- [11] M. Müller, S. Luding, and H. J. Herrmann, in *Friction, Arching and Contact Dynamics*, edited by D. E. Wolf and P. Grassberger (World Scientific, Singapore, 1997).
- [12] T. P. C. van Noije and M. H. Ernst, *Granular Matter* **1**, 57 (1998).
- [13] E. Clement and J. Rajchenbach, *Europhys. Lett.* **16**, 133 (1991).
- [14] S. Warr, G. T. H. Jacques, and J. M. Huntley, *Powder Technol.* **81**, 41 (1994); S. Warr, J. M. Huntley, and G. T. H. Jacques, *Phys. Rev. E* **52**, 5583 (1995).
- [15] A. Kudrolli, M. Wolpert, and J. P. Gollub, *Phys. Rev. Lett.* **78**, 1383 (1997).
- [16] 302 stainless steel, uniformity of diameter 0.4%, $N_{\max} = 17275$ balls constitute one monolayer at hexatic packing. The filling fraction, ρ , for N particles is N/N_{\max} .
- [17] The value for particle-plate collisions was measured directly, yet is known to be velocity dependent. For particle-particle collisions, see A. Kudrolli, M. Wolpert, and J. P. Gollub, *Phys. Rev. Lett.* **78**, 1383 (1997).
- [18] J. M. Luck and A. Mehta, *Phys. Rev. E* **48**, 3988 (1993), and references therein.
- [19] F. Melo, P. B. Umbanhowar, and H. L. Swinney, *Phys. Rev. Lett.* **75**, 3838 (1995).
- [20] A Pulnix-1040, 1008 \times 1008 pixel, 30 frames/sec (fps) camera (PULNiX America Inc., Sunnyvale, CA). Particle positions can be determined to within 0.2 pixels.
- [21] A Dalsa-CAD1, 128 \times 128 pixel, 838 fps camera (Dalsa Inc., Waterloo, ON; CANADA). Viewed from above, the trajectories of the particles are nearly straight lines between collisions. Particle positions are analyzed three images at a time. To eliminate collisions, a momentum criterion is used, $\Delta \vec{P} < \delta$, where δ is a small constant.
- [22] Visit www.physics.georgetown.edu/~granular to view the actual dynamics.
- [23] The collapse tended to form closer to the center of the cell than at the walls, presumably due to residual nonuniformity in the vibration amplitude.
- [24] O. Pouliquen, M. Nicolas, and P. D. Weidman, *Phys. Rev. Lett.* **79**, 3640 (1997).
- [25] *Bond-Orientational Order in Condensed Matter Systems*, edited by K. J. Strandburg (Springer-Verlag, New York, 1992).
- [26] D. G. Chae, F. H. Ree, and T. Ree, *J. Chem. Phys.* **50**, 1581 (1969) (interpolated for $\rho = 0.463$).
- [27] C. S. Campbell, *Ann. Rev. Fluid Mech.* **22**, 1385 (1990), and references therein.
- [28] T. A. Knight and L. V. Woodcock, *J. Phys. A* **29**, 4365 (1996).